High miR203a-3p and miR-375 expression in the airways of smokers with and without COPD

Nijnatten, J. van; Brandsma, C.A.; Steiling, K.; Hiemstra, P.S.; Timens, W.; Berge, M. van den; Faiz, A.

scientific reports

OPEN

High miR203a-3p and miR-375 expression in the airways of smokers with and without COPD

Jos van Nijnatten[1,2,3,4], Corry-Anke Brandsma[1,3], Katrina Steiling[5,6], Pieter S. Hiemstra[7], Wim Timens[1,3], Maarten van den Berge[2,3,8] & Alen Faiz[2,3,4,8]

Smoking is a leading cause of chronic obstructive pulmonary disease (COPD). It is known to have a significant impact on gene expression and (inflammatory) cell populations in the airways involved in COPD pathogenesis. In this study, we investigated the impact of smoking on the expression of miRNAs in healthy and COPD individuals. We aimed to elucidate the overall smoking-induced miRNA changes and those specific to COPD. In addition, we investigated the downstream effects on regulatory gene expression and the correlation to cellular composition. We performed a genome-wide miRNA expression analysis on a dataset of 40 current- and 22 ex-smoking COPD patients and a dataset of 35 current- and 38 non-smoking respiratory healthy controls and validated the results in an independent dataset. miRNA expression was then correlated with mRNA expression in the same patients to assess potential regulatory effects of the miRNAs. Finally, cellular deconvolution analysis was used to relate miRNAs changes to specific cell populations. Current smoking was associated with increased expression of three miRNAs in the COPD patients and 18 miRNAs in the asymptomatic smokers compared to respiratory healthy controls. In comparison, four miRNAs were lower expressed with current smoking in asymptomatic controls. Two of the three smoking-related miRNAs in COPD, miR-203a-3p and miR-375, were also higher expressed with current smoking in COPD patients and the asymptomatic controls. The other smoking-related miRNA in COPD patients, i.e. miR-31-3p, was not present in the respiratory healthy control dataset. miRNA-mRNA correlations demonstrated that miR-203a-3p, miR-375 and also miR-31-3p expression were negatively associated with genes involved in pro-inflammatory pathways and positively associated with genes involved in the xenobiotic pathway. Cellular deconvolution showed that higher levels of miR-203a-3p were associated with higher proportions of proliferating-basal cells and secretory (club and goblet) cells and lower levels of fibroblasts, luminal macrophages, endothelial cells, B-cells, amongst other cell types. MiR-375 expression was associated with lower levels of secretory cells, ionocytes and submucosal cells, but higher levels of endothelial cells, smooth muscle cells, and mast cells, amongst other cell types. In conclusion, we identified two smoking-induced miRNAs (miR-375 and miR-203a-3p) that play a role in regulating inflammation and detoxification pathways, regardless of the presence or absence of COPD. Additionally, in patients with COPD, we identified miR-31-3p as a miRNA induced by smoking. Our identified miRNAs should be studied further to unravel which smoking-induced inflammatory mechanisms are reactive and which are involved in COPD pathogenesis.

Smoking is one of the leading causes of preventable death worldwide, and despite the well-known health effects, over 15% of the world's population still smoked in 2019, according to the WHO. The smoking of cigarettes exposes the lung to more than 4000 components[1]. As a result, it is strongly associated with the development of

[1]Department of Pathology and Medical Biology, University Medical Center Groningen, The University of Groningen, Groningen, The Netherlands. [2]Department of Pulmonary Diseases, University Medical Center Groningen, The University of Groningen, Groningen, The Netherlands. [3]Groningen Research Institute for Asthma and COPD, University Medical Center Groningen, The University of Groningen, Groningen, The Netherlands. [4]Respiratory Bioinformatics and Molecular Biology, The University of Technology Sydney, Sydney, NSW, Australia. [5]Bioinformatics Program, Boston University, Boston, MA, USA. [6]Section of Pulmonary and Critical Care Medicine, Boston University School of Medicine, Boston, MA, USA. [7]Department of Pulmonology, Leiden University Medical Center, Leiden, The Netherlands. [8]These authors jointly supervised this work: Maarten van den Berge and Alen Faiz. ✉email: m.van.den.berge@umcg.nl

lung cancer[2,3] and other respiratory diseases[4,5], including chronic obstructive pulmonary disease (COPD). Characteristics of COPD are an inflammatory response in the airways and lung parenchyma, associated with progressive, irreversible airflow limitation, dyspnea, hypersecretion of mucus, and alveolar destruction, i.e., emphysema.

We have previously shown that current smoking affects levels of gene expression and DNA methylation in bronchial biopsies[6]. However, current smoking on microRNA expression in the human airway wall is not well studied so far[7,8]. MicroRNAs (miRNA) are small non-coding RNA transcripts (approximately 17–27 nucleotides long), which interact with the Argonaute protein (AGO protein) in the RNA-induced silencing complex (RISC), leading to cleavage or silencing of a target mRNA[9]. Most human protein-coding genes contain miRNA target sites[10]. A single miRNA can influence the expression of hundreds of genes[11] and regulate a broad range of biological processes, such as cell proliferation, apoptosis, and the immune system[12,13]. Because of this, deregulation of miRNA function is associated with numerous diseases, including COPD[14–16].

We also have previously shown that miRNAs play an essential role in mediating inflammatory responses and corticoid effects in asthma and COPD[17–20]. However, although several studies have assessed the impact of smoking on miRNA expression, very few have focused on the airway wall in an unbiased method[21]. Here, we investigated the influence of current smoking on miRNA expression in bronchial biopsies in two independent datasets consisting of current and ex-smoking COPD patients and current and non-smoking respiratory healthy controls to elucidate the overall smoking-induced miRNA changes and those specific to COPD. In addition, we correlated miRNA to matched mRNA expression to identify genes and pathways influenced by the miRNAs affected by smoking to investigate the downstream effects on gene expression. Finally, to investigate the relation with cellular composition, differential miRNAs expression was associated with gene signatures of specific cell populations and immunohistological staining of specific cell types in matched biopsies.

Methods

Subjects.
Affymetrix GeneChip miRNA 1.0 Array and RNA-Seq data from baseline bronchial biopsies from COPD patients and respiratory healthy controls were used for this study as described previously[22,23].

COPD patients participated in the Groningen Leiden Universities and Corticosteroids in Obstructive Lung Disease study (GLUCOLD, ClinicalTrails.gov NCT00158847) (n = 62). Respiratory healthy controls participated in the Study to Obtain Normal Values of Inflammatory Variables from Healthy Subjects (NORM study, ClinicalTrails.gov NCT00848406, n = 73). In- and exclusion criteria and more extensive characteristics of subjects participating in the GLUCOLD and NORM studies were previously described[24,25].

Briefly, for the GLUCOLD study, all patients were current or ex-smokers with > 10 pack years. Participants had irreversible airflow with postbronchodilator forced expiration volume in one second (FEV_1) < 80% predicted and postbronchodilator FEV_1/forced vital capacity (FVC) below 70%. Patients took no oral corticosteroids for at least three months before starting the study and did not use inhaled corticosteroids for at least six months prior to the study. Patients classified as ex-smokers did not smoke at least one year prior to the study.

Participants of the NORM study had normal lung function (FEV_1 > 80% and FEV_1/FVC > 70%) and no bronchial hyperresponsiveness to methacholine (PC_{20} > 16 mg/ml). Participants defined as non-smokers did not smoke during the year leading up to the study and did not smoke more than one year in total, with a total of < 0.5 packyears.

The local medical ethics committees approved all studies, and all subjects gave their written informed consent (the NORM study was approved by the ethics committee of the UMCG, and the GLUCOLD study was approved by the same committee and the ethics committee of the LUMC)[24–26]. All methods were performed in accordance with the relevant guidelines and regulations.

Statistics.
To identify differentially expressed miRNAs in bronchial biopsies of current and ex-smoking COPD patients and current and non-smoking healthy participants, we used a linear model using Limma (R-package version 3.40.6, R statistical software version 3.6). We used current smoking status as a categorical variable, adjusting for age and sex. A Benjamini–Hochberg corrected p-value (False Discovery Rate (FDR)) of < 0.05 was considered statistically significant.

We performed the identification of potential targets of differentially expressed miRNAs by directly correlating miRNA expression to normalized[27] gene expression data available from the same bronchial biopsies. We correlated significant differentially expressed miRNAs to all expressed mRNAs using the Pearson Correlation Coefficient. Significant correlations between miRNA expression levels and gene expression levels were determined using Psych (R-package version 1.8.12), and we performed a meta-analysis on the results of both studies. Significant correlations with an absolute R-value above 0.25 were considered biologically relevant.

We verified the smoking-related expression changes of the identified miRNAs using an independent miRNA dataset (Illumina HiSeq) obtained from bronchial brushings from 30 COPD patients and 30 non-COPD controls[28]. COPD was defined in this dataset by FEV_1/FVC < 70% and FEV_1 < 80% predicted and non-COPD controls were defined as FEV_1/FVC > = 70 or FEV_1/FVC < 70% and FEV_1% predicted > 80%. We used a linear model and smoking status as a categorical variable while correcting for age, sex and pack years. We analyzed the COPD and non-COPD participants separately.

miRNA predicted target approach.
We calculated the most likely target for each miRNA using miR-NAtap (R-package version 1.18.0). The default settings were used to calculate the geometric mean of ranks from the databases/algorithms PicTar, Diana, TargetScan, miRanda, and miRDB. The minimum number of sources required for a potential target was 2.
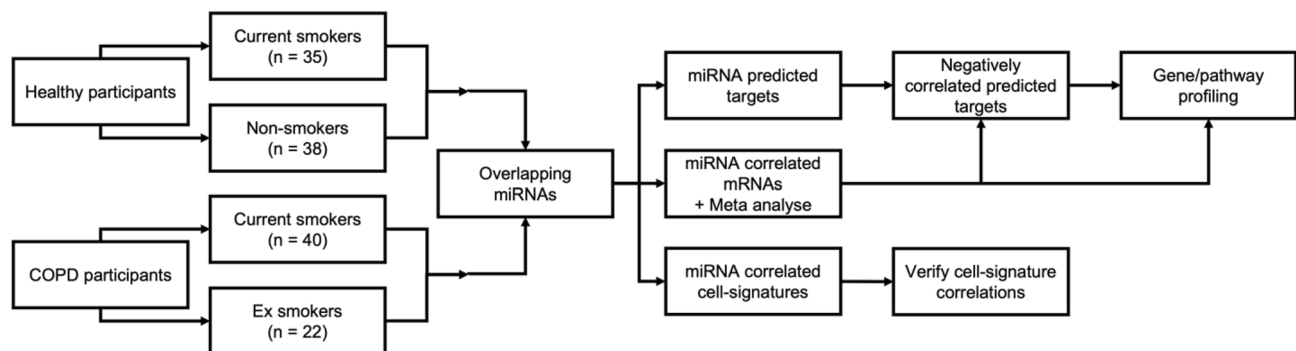
Figure 1. Flow diagram of the study approach. Two studies were used: the GLUCOLD study with current or ex-smoker COPD patients and the NORM study with current or non-smoking respiratory healthy controls. A linear regression model was used to identify smoking-associated miRNAs. The overlapping two miRNAs were used for further analysis of COPD patients. A meta-analysis of Pearson correlations was performed to identify miRNA associated mRNA. The predicted targets were obtained, and a list of negatively correlated predicted targets was compiled. Pathway analysis was performed using this list as well as on all the negative and positively correlated mRNAs. Negatively correlated predicted targets were repeated in the NORM. Additionally, miRNA expression was correlated to cell type signatures and cell populations.

	COPD patients; GLUCOLD		Respiratory Healthy controls; NORM	
	Ex-smokers	Current smokers	Non-smokers	Current smokers
N	22	40	38	35
Age mean ± SD	63 ± 8	59 ± 7	38 ± 19	41 ± 15
Sex male n (%)	20 (90.9)	33 (82.5)	20 (52.6)	20 (57.1)
FEV$_1$% predicted	55.9 ± 10.7	54.7 ± 9.5	101.4 ± 12.2	99.1 ± 9.4
FEV$_1$/FVC %	50.1 ± 9.3	46.8 ± 8.5	80.5 ± 6.6	78.0 ± 6.2
Age quit smoking mean ± SD	56 ± 10			
Cigarettes per day mean ± SD	0	18.5 ± 10.2	0	15.0 ± 7

Table 1. Patient demographics in relation to smoking status. *FEV$_1$* forced expiratory volume in 1 s, *FVC* forced vital capacity.

Pathway analysis. To predict which pathways are influenced by smoking-induced miRNAs, we performed Gene Set Enrichment Analysis (GSEA version 4.0.3) on the mRNAs positively and negatively correlated with our differentially expressed smoking-associated miRNAs. A separate analysis was done for the negatively correlated predicted target genes only. We compared the ranked lists to BioCarta and KEGG gene set databases. We then performed a meta-analysis on the pathways found in both studies and adjusted the p-value using Benjamini-Hochberg's method.

Association of miRNAs with composite scores of cell-type-specific genes based on GSVA. We used cell-type-specific gene signatures based on single-cell data for 15 cell types (activated endothelium, B-cells, basal cells, proliferating basal cells, ciliated cells, club cells and goblet cells, fibroblasts, inflammatory dendritic cells, ionocytes, luminal macrophages, mast cells, neutrophils, smooth muscle cells, and submucosal cells)[29]. We then performed Gene Set Variation Analysis (GSVA[30], R-package version 1.32.0) to calculate the composite scores for each cell type. We then correlated each composite score to relevant miRNAs using the Pearson correlation coefficient.

Evaluation of miRNAs with the presence of cell populations in matched bronchial biopsies. For the differentially expressed miRNAs, we assessed the correlation between miRNA expression and numbers of eosinophils, neutrophils, macrophages, mast cells, CD3 or CD4 or CD8 positive T-cells, and percentage of Periodic acid–Schiff stain (PAS)-positive goblet cells in paraffin-embedded bronchial biopsies from the same patients taken at the same location in the lung. These data were obtained from previously published data sets for the GLUCOLD[31] and NORM[26] studies.

A flow diagram showing the analysis approach is provided in Fig. 1.

Results

In the current study, we investigated smoking-related miRNA changes in 62 COPD patients (ex-smokers, n = 22, and current smokers, n = 40) and 73 respiratory healthy individuals (non-smokers, n = 38 and current smokers, n = 35). The subject characteristics of the two studies are presented in Table 1. There was a significant difference

miRNA id	COPD			Asymptomatic		
	Log$_2$(FC)	P-value	FDR	Log$_2$(FC)	P-value	FDR
hsa-miR-31-3p	1.18	1.16E−04	1.21E−02	NA	NA	NA
hsa-miR-203a-3p	1.50	1.17E−04	1.21E−02	0.83	2.63E−04	1.15E−02
hsa-miR-375	1.02	1.64E−04	1.21E−02	1.21	9.22E−08	9.10E−06
hsa-miR-200b-3p	0.70	2.65E−03	9.80E−02	0.49	2.28E−03	4.50E−02
hsa-miR-183-5p	0.75	8.10E−03	1.07E−01	0.84	1.37E−08	1.80E−06
hsa-miR-31-5p	0.46	1.96E−02	1.68E−01	0.65	4.10E−04	1.62E−02
hsa-miR-200c-3p	0.35	2.40E−02	1.96E−01	0.76	1.21E−05	7.94E−04
hsa-miR-200a-5p	0.55	3.06E−02	2.27E−01	0.68	1.22E−03	3.38E−02
hsa-miR-182-5p	0.35	4.16E−02	2.58E−01	0.76	3.50E−09	1.38E−06
hsa-miR-200a-3p	0.32	6.45E−02	2.87E−01	0.49	1.26E−03	3.38E−02
hsa-miR-708-5p	0.49	6.51E−02	2.87E−01	0.69	1.12E−03	3.38E−02
hsa-miR-149-5p	− 0.35	1.79E−01	4.32E−01	0.54	1.43E−03	3.38E−02
hsa-miR-181b-5p	0.15	3.65E−01	6.31E−01	0.41	1.37E−03	3.38E−02
hsa-miR-574-5p	0.24	4.21E−01	6.54E−01	0.65	1.91E−03	4.18E−02
hsa-miR-331-3p	0.14	4.79E−01	6.94E−01	0.55	4.96E−04	1.78E−02
hsa-miR-130b-3p	0.11	5.04E−01	7.22E−01	1.09	1.64E−04	9.06E−03
hsa-miR-181a-5p	0.05	7.70E−01	8.81E−01	0.47	2.17E−03	4.50E−02
hsa-miR-126-3p	− 0.03	8.99E−01	9.45E−01	− 0.38	2.65E−03	4.76E−02
hsa-miR-10b-5p	− 0.01	9.81E−01	9.91E−01	− 0.47	1.83E−04	9.06E−03
hsa-miR-3065-5p	NA	NA	NA	2.18	8.79E−09	1.74E−06
hsa-miR-3065-3p	NA	NA	NA	1.98	3.36E−06	2.66E−04
hsa-miR-126-5p	NA	NA	NA	− 0.53	1.45E−03	3.38E−02
hsa-miR-1468-5p	NA	NA	NA	− 1.10	2.62E−03	4.76E−02

Table 2. Differential expression of miRNAs for respiratory healthy controls and subjects with COPD when comparing smoking status. *FC* fold change, *FDR* false discovery rate (Benjamini Hochberg corrected p-value). Differentially expressed miRNAs with an FDR < 0.05 are shown. The table is sorted by the P-value of the COPD participants. NA's are given for probes not available in the dataset.

in sex between the COPD patients and respiratory healthy individuals (Chi-Squared p-value = 3E−4), as well as a significant difference in age (Mann–Whitney U p-value = 2E−11).

Changes in miRNA expression associated with current smoking. We identified three miRNAs (miR-31-3p, miR-203a-3p, and miR-375) differentially expressed between current- and ex-smoking COPD patients (FDR < 0.05). All three miRNAs showed a higher level of expression in current- compared to ex-smokers (Table 2). A volcano plot and heatmap are depicted in Fig. 2A,B.

We next repeated this analysis in respiratory healthy individuals. A total of 22 miRNAs were differentially expressed in the current- versus non-smokers (FDR < 0.05). Of these, 18 miRNAs showed a higher expression level in current smokers than non-smokers, while four were lower expressed (Table 2). A volcano plot and heatmap are depicted in Fig. 2C,D, respectively.

Two miRNAs, miR-375 and miR-203a-3p, were associated with current smoking in the same direction in both COPD patients and respiratory healthy controls (Fig. 2E–G).

MiR-31-3p, the third smoking-associated miRNA in the COPD patients, was not present in the respiratory healthy small-RNA-seq dataset.

We validated our findings in an independent dataset of epithelial brushes. We confirmed higher miR-375 expression in current- than ex-smokers in COPD and non-COPD, but no effect of smoking status on miR-203a-3p or miR-31-3p. (Supplementary Table S4).

Associations between changes in miRNA expression and mRNA expression. To identify potential genes and pathways that are regulated by the three smoking-associated miRNAs, we used two different methods: (1) we investigated the global effects of the miRNAs by doing direct correlations with all expressed genes in the same biopsies, and (2) we investigated the direct effects by focusing on the negatively correlated predicted targets for each miRNA.

For the first analysis, we examined whether miR-375, miR-203a-3p and miR-31-3p affected the expression of mRNA transcripts in each study separately and then performed a meta-analysis for the miRNAs present in both studies (miR-375 and miR-203a-3p). Here, we identified 983 significant negatively correlated genes for miR-203a-3p (FDR < 0.05), and 2254 positively correlated genes. We found 2442 significantly negatively correlated genes for miR-375 and 865 positively correlated genes, and we found 1106 significant negative correlations for miR-31-3p and 1029 positive correlations (Table S1). The top 3 most strongly correlated genes (*PDGFD*, *ARL4C* and *MBNL1*) of both miR-375 and miR-203a-3p are shown in Fig. 3C–H. Gene functions are described in Table 3.
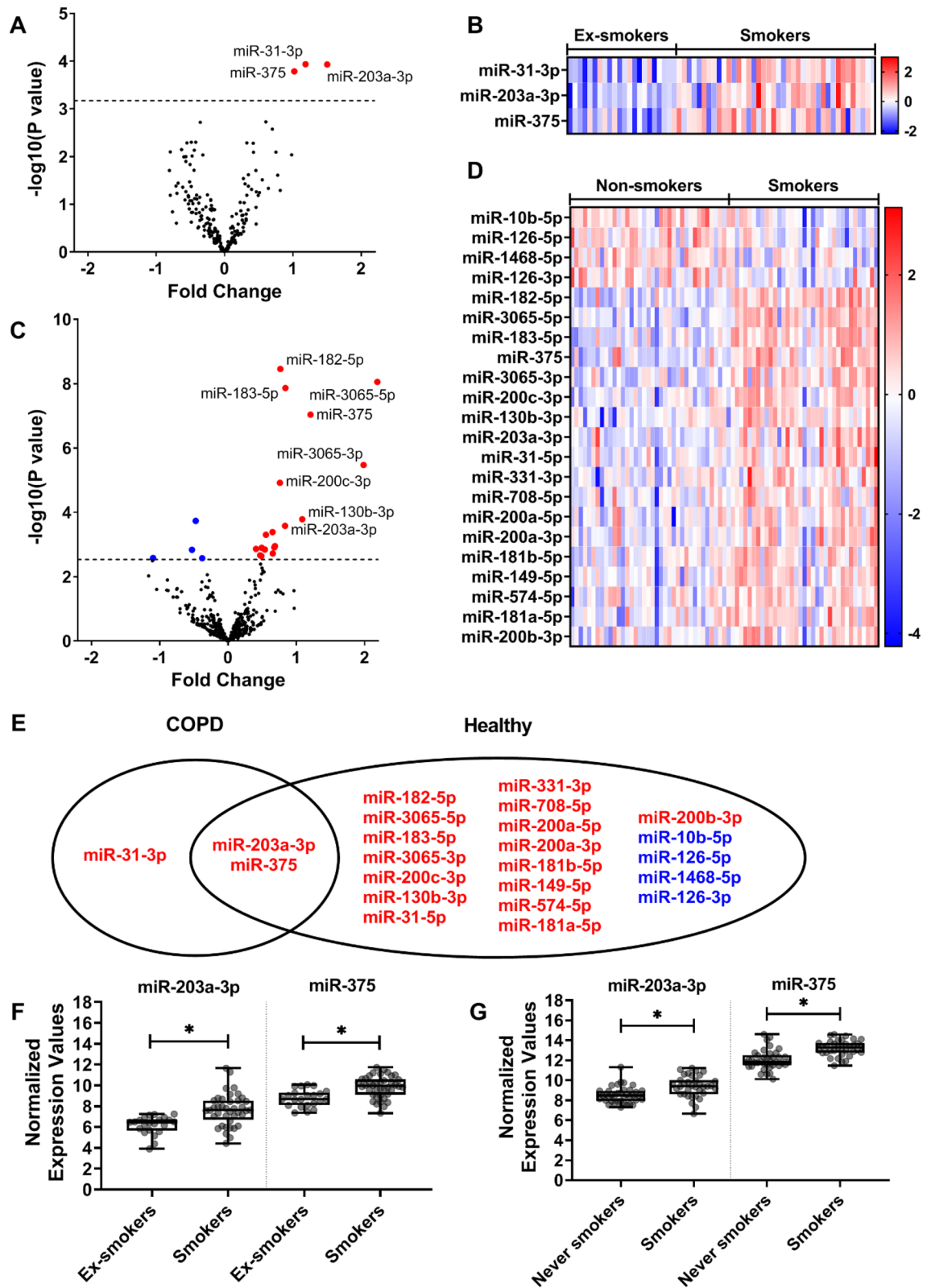
Figure 2. Differentially expressed microRNAs (miRNAs) when comparing smoking status in patients with COPD and respiratory healthy controls. Volcano plot (**A**) shows changes in expression levels of 220 miRNAs in patients with COPD (n = 62). Heat map (**B**) shows expression changes of the three significantly differentially expressed miRNAs in COPD patients. Volcano plot (**C**) shows changes in the expression of 395 miRNAs in respiratory healthy controls (n = 73). Heat map (**D**) shows expression changes of the 22 significantly differentially expressed miRNAs in respiratory healthy controls. Venn diagram (**E**) shows the overlap between significantly differentially expressed miRNAs in COPD patients compared to respiratory healthy controls. Boxplot (**F**) shows the normalized expression values of the miRNAs miR-203a-3p and miR-375 per smoking group in the COPD patients, and boxplot (**G**) shows the normalized expression values for the same miRNAs in the respiratory healthy controls. Red indicates an increase in expression, whereas blue indicates a decrease in expression. A false discovery rate (FDR) cut-off of 0.05 was used.
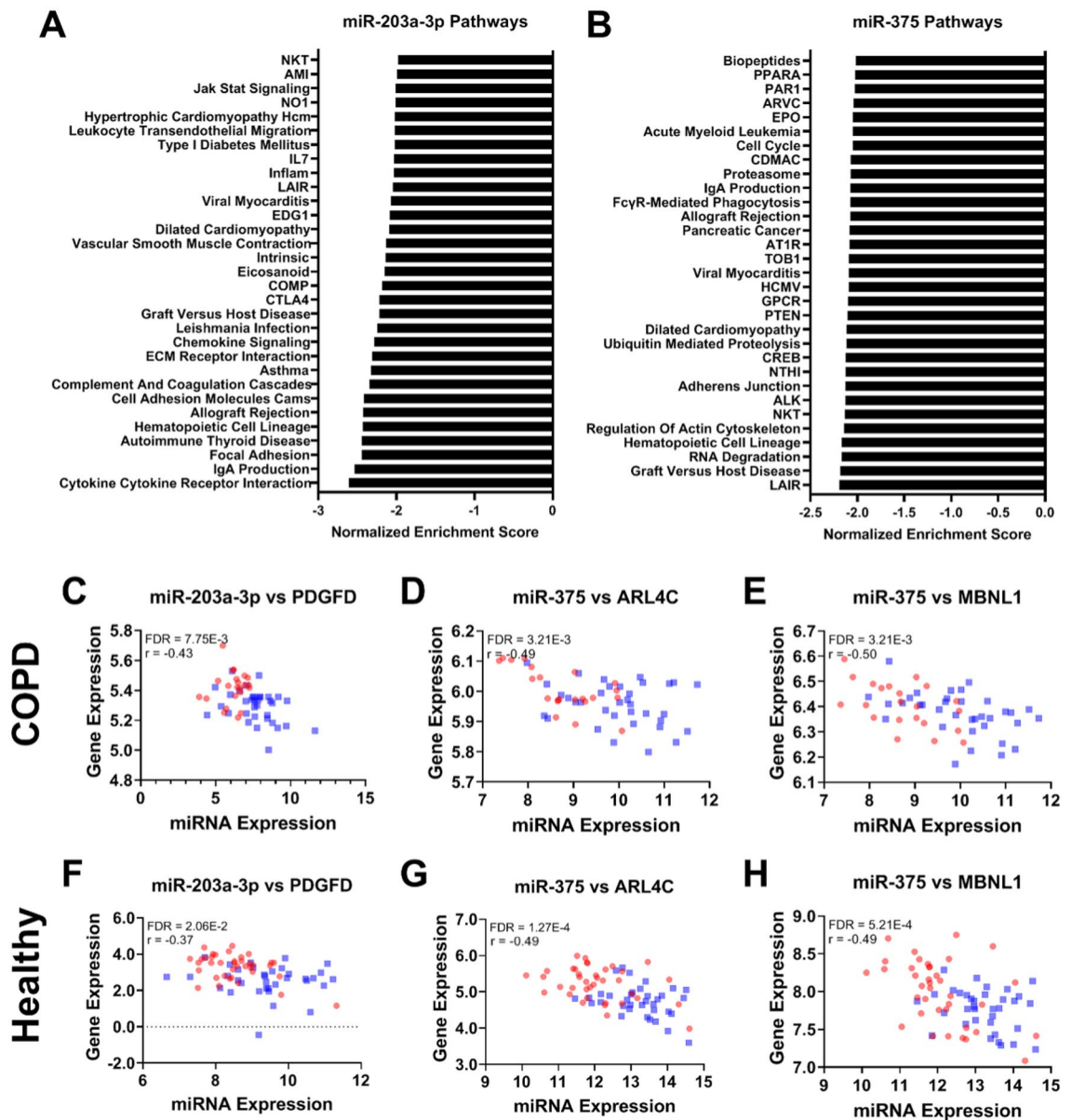
Figure 3. Significant pathway negatively enrichment by miRNA-203a-3p and miR-375 and correlation of aforementioned miRNAs with genes in both COPD patients as well as respiratory healthy controls, excluding correlations that were considered not biologically relevant due to a low r-value. (**A**) Enriched pathways affected by miR-203a-3p in COPD patients. (**B**) The enriched pathways affected by miR-375 in COPD patients. Scatter plots (**C**–**E**) show the correlation between miRNA expression and gene expression levels in COPD patients for all significant negatively correlated predicted targets; miR-203a-3p and *PDGFD*, miR-3758, and *ARL4C*, and miR-375 expression and *MBNL1*, respectively. Smoking participants are shown in blue, ex-, and non-smokers are shown in red. Scatter plots (**F**–**H**) show the correlation between miRNA expression and gene expression levels in respiratory healthy controls between miR-203a-3p and *PDGFD*, miR-375, and *ARL4C*, and mir-375 and *MBNL1*, respectively.

Correlation with predicted target genes. For the targeted analysis, we focused on negatively correlated predicted targets for miR-203a-3p, miR-375 and miR-31-3p. First, predicted targets were identified using miR-NAtap, and then the overlap was taken from the negatively correlated genes from the previous analysis.

Of the 983 genes negatively correlated with miR-203a-3p, two genes were also predicted targets; *PDGFD*, previously associated with fibroblast proliferation and survival, and *EBF3,* previously associated with B cell differentiation and cell survival through apoptosis and cell cycle arrest[32–34].

Of the 2442 genes negatively correlated to miR-375, 18 were also predicted targets; *ZNF385D, MBNL1, ARL4C, PDE5A, MMD, APBB2, LDHB, HAS2, CXCL12, CNIH4, APBB1IP, DTHD1, LST1, RLF, SLC16A2, TCF12, TRAPPC6B* and *WBP1L* (Fig. 3C–H).

For miR-31-3p, we found that 14 of the 1106 negatively correlated genes were also predicted targets; *NFATC2, PLCB1, PDE5A, RXFP1, DLC1, TOX, C1QTNF7, PIK3CG, IL15, DIRAS3, WASF3, LGI2, KCNIP2* and *TMOD2.*

miRNA id	Gene symbol	r (COPD)	r (Healthy)	Meta-analysis FDR	Gene function
miR-375	ARL4C	− 0.49	− 0.52	1.45E−06	Involved in tumorigenesis in lung[41,42]
miR-375	MBNL1	− 0.50	− 0.49	5.52E−06	Tumorigenesis via an isoform[43], regulates alternative splicing[44]
miR-375	SLC16A2	− 0.30	− 0.53	3.71E−05	Transportation of diiodothyronine, thyroxine and triiodothyronine[45]
miR-375	RLF	− 0.35	− 0.45	2.75E−04	Tumorgenesis[46]
miR-203a-3p	PDGFD	− 0.43	− 0.37	9.58E−04	Fibroblast proliferation and survival, associated with adrenal suppression[32,33]
miR-375	TCF12	− 0.34	− 0.39	1.86E−03	Tumorgenesis in several cancers. Cell differentiation, repression of E-cadherin, cell development, differentiation of lymphocytes[47–51]
miR-375	WBP1L	− 0.25	− 0.43	2.20E−03	Regulates CXCR4 signalling in leukocytes and alters B-cell development[36]
miR-375	PDE5A	− 0.49	− 0.29	3.13E−03	Regulates cyclic GMP, intercellular messengers that mediate the effects of extracellular signalling molecules[52,53]. Regulates pulmonary hypertension
miR-375	APBB2	− 0.42	− 0.32	3.72E−03	Adapter protein, signal transduction[54,55]
miR-375	ZNF385D	− 0.54	− 0.24	4.87E−03	
miR-375	CNIH4	− 0.39	− 0.33	5.13E−03	Located in the secretory pathway, it promotes the exit of GPCRs[56]
miR-375	MMD	− 0.45	− 0.27	7.77E−03	Macrophages activation[57], highly expressed in non-small cell lung cancer[58]
miR-375	HAS2	− 0.40	− 0.29	9.63E−03	Regulates cell adhesion, extracellular matrix formation, tumorigenesis[59,60]
miR-375	CXCL12	− 0.39	− 0.29	1.03E−02	Chemoattractant for T-lymphocytes and monocytes[61]
miR-375	LDHB	− 0.41	− 0.27	1.35E−02	Involved in tumorigenesis[62], a subunit of lactate dehydrogenase
miR-375	TRAPPC6B	− 0.28	− 0.29	3.73E−02	Vesicle transport[63], involved in the secretory pathway[64]
miR-375	APBB1IP	− 0.33	− 0.26	4.02E−02	Adapter protein, signal transduction[54,55]
miR-203a-3p	EBF3	− 0.58	− 0.10	4.22E−02	B-cell differentiation, bone development, neurogenesis and tumour suppressor via cell cycle arrest and apoptosis[34]
				FDR	
miR-31-3p	NFATC2	− 0.58		2.74E−06	nuclear factor of activated T cells—translocates to the nucleus upon T cell receptor (TCR)—immune response[65,66]
miR-31-3p	PLCB1	− 0.50		8.61E−05	intracellular transduction of many extracellular signals
miR-31-3p	PDE5A	− 0.48		1.40E−04	cAMP binding—smooth muscle relaxation in the cardiovascular system[67,68]
miR-31-3p	RXFP1	− 0.48		1.43E−04	
miR-31-3p	DLC1	− 0.47		2.52E−04	GAP family proteins participate in signalling pathways that regulate cell processes involved in cytoskeletal changes[69].—angiogenesis[70]
miR-31-3p	TOX	− 0.45		4.06E−04	HMG box DNA binding domain.—chromatin assembly, transcription and replication[71]—T-cell development[72]
miR-31-3p	C1QTNF7	− 0.45		4.54E−04	
miR-31-3p	PIK3CG	− 0.42		1.15E−03	immune response, proliferation and survival[73,74]
miR-31-3p	IL15	− 0.40		1.98E−03	regulates T and natural killer cell activation and proliferation[75]
miR-31-3p	DIRAS3	− 0.40		2.24E−03	Inhibits RAS/MAPK signalling[76]
miR-31-3p	WASF3	− 0.38		4.02E−03	transduce signals that involve changes in cell shape, motility or function[77]
miR-31-3p	LGI2	− 0.37		4.53E−03	
miR-31-3p	KCNIP2	− 0.37		4.54E−03	Voltage-gated potassium channels
miR-31-3p	TMOD2	− 0.36		5.48E−03	actin regulatory protein[77]
miR-31-3p	RAB3C	− 0.35		8.29E−03	

Table 3. Selective literature of predicted target genes that were negatively correlated to miR-203a-3p, miR-375 and miR-31-3p, whilst significant after our meta-analysis (miR-203a-3p and miR-375) or FDR significant (miR-31-3p) after correlation.

Pathways affected by miRNA expression that change with current smoking patients. To investigate the pathways influenced by changes in miRNA levels, we performed pathway analysis on (1) all genes of which the expression correlated to the identified miRNAs, for a global effect (Fig. 3A,B), and (2) the significantly negatively correlated predicted targets of the miRNAs, for a direct effect of these miRNAs.

For miR-203a-3p, we found a higher expression associated with genes involved in cellular protection (xenobiotic and glutathione metabolism pathways), cellular repair (cell cycle, citrate cycle pathways), and protease pathway, as well as negative associations with pro-inflammatory pathways. In addition, the MAPK signalling pathway was negatively associated with miR-203a-3p associated genes in COPD patients (Table 4).

We found a global positive effect of genes associated with a higher expression of miR-375 on olfactory transduction, glycan biosynthesis and linoleic acid metabolism, and adverse effects on pro-inflammatory pathways in COPD patients, for example, via the cytokine-cytokine receptor integration pathway (Table 4).

A higher expression of miR-31-3p had positive associations with genes involved in pathways related to xenobiotic metabolism, cellular repair and linoleic acid metabolism, as well as negative associations with genes involved in pro-inflammatory pathways.

miRNA	Gene sets	COPD			Asymptomatic			Total genes
		NES	FWER P-value	Core-enriched genes	NES	FWER P-value	Core-enriched genes	
miR-203a-3p	Cytokine–cytokine Receptor interaction	− 2.58	0.00E+00	122	− 2.78	0.00E+00	125	253
	Intestinal immune Network For IgA production	− 2.53	0.00E+00	36	− 2.92	0.00E+00	26	45
	Focal adhesion	− 2.46	0.00E+00	78	− 2.27	8.00E−03	88	197
	Systemic lupus Erythematosus	− 2.43	0.00E+00	27	− 2.96	0.00E+00	31	50
	Autoimmune thyroid disease	− 2.43	0.00E+00	31	− 2.71	0.00E+00	22	49
	Hematopoietic cell lineage	− 2.42	0.00E+00	51	− 2.80	0.00E+00	49	83
	Asthma	− 2.42	0.00E+00	14	− 2.54	0.00E+00	14	28
	Cell adhesion Molecules cams	− 2.41	0.00E+00	60	− 2.58	0.00E+00	61	126
	Allograft rejection	− 2.41	0.00E+00	26	− 2.99	0.00E+00	23	35
	Complement and coagulation cascades	− 2.32	0.00E+00	26	− 2.18	1.60E−02	36	67
	ECM receptor interaction	− 2.29	0.00E+00	40	− 2.04	4.20E−02	43	83
	Chemokine signaling	− 2.27	0.00E+00	72	− 2.21	1.30E−02	53	179
	Leishmania infection	− 2.25	0.00E+00	37	− 2.84	0.00E+00	26	65
miR-375	Ribosome	− 3.05	0.00E+00	53	− 2.72	0.00E+00	65	75
	Leishmania infection	− 2.75	0.00E+00	35	− 1.93	1.20E−02	38	65
	Focal adhesion	− 2.74	0.00E+00	105	− 2.04	0.00E+00	103	197
	Il2rb	− 2.71	0.00E+00	25	− 2.20	0.00E+00	26	37
	MET	− 2.66	0.00E+00	25	− 2.08	0.00E+00	22	33
	B cell receptor signaling	− 2.62	0.00E+00	44	− 1.84	1.03E−01	40	75
	PDGF	− 2.60	0.00E+00	20	− 1.94	1.20E−02	23	28
	GH	− 2.58	0.00E+00	16	− 2.13	0.00E+00	20	27
	FCER1	− 2.58	0.00E+00	25	− 1.93	1.20E−02	29	39
	GLEEVEC	− 2.51	0.00E+00	18	− 1.94	1.10E−02	15	23
	Renal cell carcinoma	− 2.51	0.00E+00	37	− 2.03	1.00E−03	39	66
	TCR	− 2.49	0.00E+00	29	− 1.98	3.00E−03	33	44
	CTCF	− 2.48	0.00E+00	18	− 2.05	0.00E+00	15	24
	Integrin	− 2.46	0.00E+00	22	− 2.06	0.00E+00	21	34
miR-31-3p	Hematopoietic cell lineage	− 2.56	0.00E+00	44				83
	Intestinal immune network For IgA production	− 2.56	0.00E+00	24				46
	Cytokine–cytokine Receptor interaction	− 2.55	0.00E+00	110				254
	Systemic lupus Erythematosus	− 2.46	0.00E+00	29				50
	Focal adhesion	− 2.44	0.00E+00	74				197
	Leishmania infection	− 2.43	0.00E+00	28				66
	ECM receptor interaction	− 2.39	0.00E+00	45				83
	Cell adhesion Molecules cams	− 2.31	0.00E+00	51				128
	Chemokine signaling Pathway	− 2.28	0.00E+00	65				180
	Autoimmune thyroid disease	− 2.26	0.00E+00	35				49
	Asthma	− 2.26	0.00E+00	18				28
	Allograft rejection	− 2.25	0.00E+00	28				35
	LAIR pathway	− 2.24	0.00E+00	13				16

Table 4. Significant gene sets negatively affected by the identified miRNAs in COPD patients and asymptomatic participants. Only the top pathways with a family-wise error rate < 0.05 in the COPD patients are shown. *NES* normalized enrichment score, *FWER P-value* family-wise error rate p-value.

Relation between cell-type composition and genes associated with miRNAs. Two methods were used to assess potential effects of cell-type composition on the expression of the miRNA-associated genes, i.e. GSVA based on single-cell gene signatures derived from a publically available dataset and correlation analysis with inflammatory cell counts assessed in adjacent biopsies of the same patients.

With the GSVA analysis, we found a significant negative correlation between miR-203a-3p expression and cell type composite scores of single-cell signatures for fibroblasts, luminal macrophages, endothelial cells, mast cells, smooth muscle cells, B-cells, submucosal cells and inflammatory dendric cells. In contrast, we found a positive association of this miRNA with proliferating basal cells and club and goblet cells with current smoking in both COPD patients and respiratory healthy controls.

For miR-375, we found a negative correlation with cell type composite scores for endothelial cells, smooth muscle cells, mast cells, fibroblasts, basal cells and luminal macrophages., and a positive correlation with club

and goblet cells, ionocytes and submucosal cells in both studies (Supplementary Tables S2 and S3). Activated endothelium, fibroblasts, luminal macrophages, mast cells and smooth muscle cells GSVA composite scores were negatively associated with mir-31-3p while proliferating basal cells and club and goblet cells were positively associated.

In addition, we correlated the miRNA expression profiles to cell counts of eosinophils, neutrophils, macrophages, mast cells, CD3 + , CD4 + or CD8 + T-cells, CD20 + B-cells, and percentage of PAS staining positive mucus in the COPD study. We found a negative correlation between eosinophils and miR-203a-3p expression and a positive correlation between miR-31-3p and epithelial cells, but no association with miR-375 (data not shown).

Discussion

In the current study, we identified two miRNAs (miR-203a-3p and miR-375) that are significantly higher expressed with current smoking in COPD patients and respiratory healthy subjects, indicating a common effect of smoking regardless of disease status. Additionally, we found that miR-31-3p is associated with current smoking only in COPD patients.

We found that miR-375 is higher expressed in bronchial biopsies of current-smoking COPD patients and respiratory healthy controls, and we validated this finding in an independent dataset. We identified 18 predicted target genes that decrease with increased miR-375 expression. These included *TCF12, WBP1L, CXCL12, MMD, and LST1* that were previously associated with inflammation via T-cell precursor differentiation[35], altering B-cell development[36], chemotaxis[57], differentiation of monocytes to macrophages[53], or differentiation of other cells[59]. These predicted target genes were not enriched in one specific pathway. However, our global miRNA pathway analysis showed that genes associated with miR-375 are lower expressed in pro-inflammatory pathway activity, such as the IL2RB and B-cell receptor signalling pathway. We continued our investigation using cellular deconvolution and found that higher levels of miR-375 are associated with lower levels of basal cells, fibroblasts, mast cells, smooth muscle cells, endothelial cells and luminal macrophages and higher levels of secretory cells, submucosal cells and ionocytes. In contrast, no association was found with inflammatory cell populations as determined histologically. As we consistently find miR-375 being increased by smoke across all datasets and a positive correlation between miR-375 with secretory cells, this may indicate cell-specific expression in secretory cells as it is well established that the levels of secretory cells are higher in current smokers[37]. The high number of genes and pathways related to inflammation changed by miR-375, but the lack of correlation to gene signatures typical for inflammatory cells might indicate an increased activation of inflammatory cells caused by miR-375 rather than a change in cell numbers or composition.

We showed that miR-203a-3p is more highly expressed in bronchial biopsies of current- compared to ex-smokers with COPD and in current- versus non-smoking respiratory healthy subjects. Furthermore, two negatively correlated predicted targets of miR-203a-3, *EBF3* and *PDGFD,* were involved in cell cycle arrest and apoptosis[31] and fibroblast proliferation[29,30], respectively. Therefore, the lower *EBF3* and *PDGFD* in response to smoking in association with miRNA-203a-3p by smoking potentially indicates a protective response and stimulation of repair as a response to cigarette smoke. In addition, we found that genes associated with xenobiotic metabolism were positively correlated with miR-203a-3p, suggesting that this miRNA facilitates the metabolism of harmful particles in cigarette smoke[38]. Additionally, we found that genes involved in pro-inflammatory pathways (e.g. cytokine-cytokine receptor interaction, IgA production and chemokine signalling) were negatively correlated with miR-203a-3p, suggesting an anti-inflammatory effect for this miRNA. We associated these microRNAs with cell signatures to assess whether a change in cell populations may drive the smoking-induced increase in miR-203a-3p expression. We found higher smoking-induced expression of miR-203a-3p associated with lower proportions of fibroblasts, luminal macrophages, endothelial cells, mast cells, smooth muscle cells, B-cells, inflammatory dendritic cells, and submucosal cells and higher proportions of secretory cells (club and goblet cells) and proliferating basal cells. Therefore, it could be speculated that miR-203a-3p might play a role in the basal cell's differentiation towards secretory cells, leading to more mucus production in smokers or that this miRNA is selectively expressed in secretory cells. This, however, has now only been demonstrated in biopsies and requires further investigation in isolated cells to see the relationship of this miRNA with basal cell differentiation towards secretory cells, with and without smoke exposure.

MiR-31-3p was higher in current- compared to ex-smoking COPD patients, and this miRNA was not found in the respiratory healthy control dataset. We found 14 predicted target genes that decreased with an increase of miR-31-3p. Among these genes was *PDE5A*, which was involved in smooth muscle contraction and relaxation, as well as cell proliferation, cell signalling and included pro-inflammatory w Inhibition of *PDE5A* is involved in preventing tobacco smoke-induced emphysema[39], suggesting a protective role of this miRNA in current smokers with COPD as an attempt to limit the harmful effects of smoking[40]. In a previous study, it was shown that *PDE5A* was decreased after smoke exposure in lung tissue of healthy individuals[40]. The higher expression of miR-31-3p could suppress *PDE5A* expression even further in patients with COPD.

There were some limitations to the current study. As the miRNAs expression in the healthy group were conducted on different platforms, these miRNAs were not directly comparable. This may have led to the lack of expression of miRNA-31-3p in the healthy cohort. However, as the healthy cohort was conducted with small-RNA-Seq, it should have been picked up when present, and therefore we are confident in the current results. As a strength of the study, we were able to directly correlate the miRNA to matched expression data in the same subject allowing for the identification of direct miRNA-target gene interactions. Predicted targets for the miRNAs were identified using miRNAtap, which relies on algorithms and databases. However, as these are only predictions and not necessarily accurate, having the paired gene expression and miRNA expression needs additional confirmation of the associations.

In conclusion, we found two miRNAs, miR-203a-3p and miR-375, that are upregulated in bronchial biopsies of smokers compared to ex- and non-smokers in both COPD and respiratory healthy controls. These miRNAs play a role in the detoxification and inflammatory response to smoke response. In addition, we identified that miR-31-3p was upregulated only in current smokers versus ex-smokers with COPD. miR-31-3p might have a protective role via decreasing *PDE5A* expression and thus smoke-induced emphysema. We propose that our identified miRNAs are candidates for future studies aimed at unravelling which smoking-induced inflammatory mechanisms are mainly reactive and which are involved in COPD pathogenesis.

References

1. Hoffmann, D., & Hoffmann, I. *Letters to the Editor—Tobacco smoke components.* Beiträge zur Tabakforschung International/Contributions to Tobacco Research **18**(1), p. 49–52 (1998).
2. Hecht, S. S. Cigarette smoking and lung cancer: Chemical mechanisms and approaches to prevention. *Lancet Oncol.* **3**(8), 461–469 (2002).
3. Govindan, R. *et al.* Genomic landscape of non-small cell lung cancer in smokers and never-smokers. *Cell* **150**(6), 1121–1134 (2012).
4. Klareskog, L., Padyukov, L. & Alfredsson, L. Smoking as a trigger for inflammatory rheumatic diseases. *Curr. Opin. Rheumatol.* **19**(1), 49–54 (2007).
5. Andres, S. A. *et al.* Interaction between smoking history and gene expression levels impacts survival of breast cancer patients. *Breast Cancer Res. Treat.* **152**(3), 545–556 (2015).
6. Nedeljkovic, I. *et al.* COPD GWAS variant at 19q13.2 in relation with DNA methylation and gene expression. *Hum. Mol. Genet.* **27**(2), 396–405 (2017).
7. Perdomo, C. *et al.* MicroRNA 4423 is a primate-specific regulator of airway epithelial cell differentiation and lung carcinogenesis. *Proc. Natl. Acad. Sci. USA* **110**(47), 18946–18951 (2013).
8. Schembri, F. *et al.* MicroRNAs as modulators of smoking-induced gene expression changes in human airway epithelium. *Proc. Natl. Acad. Sci. USA* **106**(7), 2319–2324 (2009).
9. Hammond, S. M. *et al.* An RNA-directed nuclease mediates post-transcriptional gene silencing in Drosophila cells. *Nature* **404**(6775), 293–296 (2000).
10. Friedman, R. C. *et al.* Most mammalian mRNAs are conserved targets of microRNAs. *Genome Res.* **19**(1), 92–105 (2009).
11. Lim, L. P. *et al.* Microarray analysis shows that some microRNAs downregulate large numbers of target mRNAs. *Nature* **433**(7027), 769–773 (2005).
12. Podshivalova, K. & Salomon, D. R. MicroRNA regulation of T-lymphocyte immunity: modulation of molecular networks responsible for T-cell activation, differentiation, and development. *Crit. Rev. Immunol.* **33**(5), 435–476 (2013).
13. Hwang, H. W. & Mendell, J. T. MicroRNAs in cell proliferation, cell death, and tumorigenesis. *Br. J. Cancer* **94**(6), 776–780 (2006).
14. Lacedonia, D. *et al.* Expression profiling of miRNA-145 and miRNA-338 in serum and sputum of patients with COPD, asthma, and asthma-COPD overlap syndrome phenotype. *Int. J. Chron. Obstruct. Pulmon. Dis.* **12**, 1811–1817 (2017).
15. Ezzie, M. E. *et al.* Gene expression networks in COPD: microRNA and mRNA regulation. *Thorax* **67**(2), 122–131 (2012).
16. Kim, W. J. *et al.* Altered miRNA expression in lung tissues of patients with chronic obstructive pulmonary disease. *Mol. Cell. Toxicol.* **13**(2), 207–212 (2017).
17. Faiz, A. *et al.* Effect of long-term corticosteroid treatment on microRNA and gene-expression profiles in COPD. **53**(4), 1801202 (2019).
18. Faiz, A., et al., Profiling of healthy and asthmatic airway smooth muscle cells following interleukin-1β treatment: a novel role for CCL20 in chronic mucus hypersecretion. **52**(2), 1800310 (2018).
19. Osei, E.T., et al., miR-146a-5p plays an essential role in the aberrant epithelial–fibroblast cross-talk in COPD. **49**(5), 1602538 (2017).
20. Boudewijn, I. M. *et al.* A novel role for bronchial MicroRNAs and long noncoding RNAs in asthma remission. *Am. J. Respir. Crit. Care Med.* **202**(4), 614–618 (2020).
21. Conickx, G., et al., microRNA profiling in lung tissue and bronchoalveolar lavage of cigarette smoke-exposed mice and in COPD patients: a translational approach. **7**(1), 12871 (2017).
22. Faiz, A., et al., Effect of long-term corticosteroid treatment on microRNA and gene-expression profiles in Chronic Obstructive Pulmonary Disease. *Eur. Respir. J.* 1801202 (2019).
23. Tasena, H., et al., microRNA–mRNA regulatory networks underlying chronic mucus hypersecretion in COPD. **52**(3), 1701556 (2018).
24. Lapperre, T. S. *et al.* Smoking cessation and bronchial epithelial remodelling in COPD: A cross-sectional study. *Respir. Res.* **8**(1), 85 (2007).
25. Hoonhorst, S. J. M. *et al.* Advanced glycation endproducts and their receptor in different body compartments in COPD. *Respir. Res.* **17**(1), 46 (2016).
26. Ong, J. *et al.* Age-related gene and miRNA expression changes in airways of healthy individuals. *Sci. Rep.* **9**(1), 3765 (2019).
27. Law, C. W. *et al.* voom: Precision weights unlock linear model analysis tools for RNA-seq read counts. *Genome Biol.* **15**(2), R29 (2014).
28. Steiling, K. *et al.* A dynamic bronchial airway gene expression signature of chronic obstructive pulmonary disease and lung function impairment. *Am. J. Respir. Crit. Care Med.* **187**(9), 933–942 (2013).
29. Vieira Braga, F. A. *et al.* A cellular census of human lungs identifies novel cell states in health and in asthma. *Nat. Med.* **25**(7), 1153–1163 (2019).
30. Hanzelmann, S., Castelo, R. & Guinney, J. GSVA: Gene set variation analysis for microarray and RNA-seq data. *BMC Bioinformatics* **14**, 7 (2013).
31. van den Berge, M. *et al.* Airway gene expression in COPD is dynamic with inhaled corticosteroid treatment and reflects biological pathways associated with disease activity. *Thorax* **69**(1), 14 (2014).
32. Warshamana, G. S. *et al.* Dexamethasone activates expression of the PDGF-alpha receptor and induces lung fibroblast proliferation. *Am. J. Physiol.* **274**(4), L499-507 (1998).
33. Hawcutt, D. B. *et al.* Susceptibility to corticosteroid-induced adrenal suppression: A genome-wide association study. *Lancet Respir. Med.* **6**(6), 442–450 (2018).
34. Boller, S. & Grosschedl, R. The regulatory network of B-cell differentiation: A focused view of early B-cell factor 1 function. *Immunol. Rev.* **261**(1), 102–115 (2014).
35. Braunstein, M. & Anderson, M. K. HEB-deficient T-cell precursors lose T-cell potential and adopt an alternative pathway of differentiation. *Mol. Cell Biol.* **31**(5), 971–982 (2011).

36. Borna, S. *et al.* Transmembrane adaptor protein WBP1L regulates CXCR4 signalling and murine haematopoiesis. *J. Cell. Mol. Med.* **24**(2), 1980–1992 (2020).
37. Cerveri, I. & Brusasco, V. Revisited role for mucus hypersecretion in the pathogenesis of COPD. *Eur. Respir. Rev.* **19**(116), 109–112 (2010).
38. Meyer, U. A. Overview of enzymes of drug metabolism. *J. Pharmacokinet. Biopharm.* **24**(5), 449–459 (1996).
39. Seimetz, M. *et al.* Cigarette smoke-induced emphysema and pulmonary hypertension can be prevented by phosphodiesterase 4 and 5 inhibition in mice. *PLoS ONE* **10**(6), 9327 (2015).
40. Zuo, H. *et al.* Cigarette smoke exposure alters phosphodiesterases in human structural lung cells. *Am. J. Physiol. Lung. Cell. Mol. Physiol.* **318**(1), L59–L64 (2020).
41. Fujii, S. *et al.* Arl4c expression in colorectal and lung cancers promotes tumorigenesis and may represent a novel therapeutic target. *Oncogene* **34**(37), 4834–4844 (2015).
42. Kimura, K. *et al.* ARL4C is associated with initiation and progression of lung adenocarcinoma and represents a therapeutic target. *Cancer Sci.* **111**(3), 951–961 (2020).
43. Tabaglio, T., et al. MBNL1 alternative splicing isoforms play opposing roles in cancer. *Life Sci. Alliance* **1**(5), 157 (2018).
44. Goers, E. S. *et al.* MBNL1 binds GC motifs embedded in pyrimidines to regulate alternative splicing. *Nucleic Acids Res.* **38**(7), 2467–2484 (2010).
45. Jansen, J. *et al.* Functional analysis of monocarboxylate transporter 8 mutations identified in patients with X-linked psychomotor retardation and elevated serum triiodothyronine. *J. Clin. Endocrinol. Metab.* **92**(6), 2378–2381 (2007).
46. Makela, T. P. *et al.* Intrachromosomal rearrangements fusing L-myc and rlf in small-cell lung cancer. *Mol. Cell Biol.* **11**(8), 4015–4021 (1991).
47. Chen, W. S. *et al.* Secreted heat shock protein 90alpha (HSP90alpha) induces nuclear factor-kappaB-mediated TCF12 protein expression to down-regulate E-cadherin and to enhance colorectal cancer cell migration and invasion. *J. Biol. Chem.* **288**(13), 9001–9010 (2013).
48. Lee, C. C. *et al.* TCF12 protein functions as transcriptional repressor of E-cadherin, and its overexpression is correlated with metastasis of colorectal cancer. *J. Biol. Chem.* **287**(4), 2798–2809 (2012).
49. L'Abbate, A. *et al.* t(15;21) translocations leading to the concurrent downregulation of RUNX1 and its transcription factor partner genes SIN3A and TCF12 in myeloid disorders. *Mol. Cancer* **14**, 211 (2015).
50. Uittenbogaard, M. & Chiaramello, A. Expression of the bHLH transcription factor Tcf12 (ME1) gene is linked to the expansion of precursor cell populations during neurogenesis. *Gene Exp. Patterns* **1**(2), 115–121 (2002).
51. Mesman, S. & Smidt, M. P. Tcf12 is involved in early cell-fate determination and subset specification of midbrain dopamine neurons. *Front. Mol. Neurosci.* **10**, 353 (2017).
52. Schudt, C. *et al.* Therapeutic potential of selective PDE inhibitors in asthma. *Pulm. Pharmacol. Ther.* **12**(2), 123–129 (1999).
53. Movsesian, M. A. Beta-adrenergic receptor agonists and cyclic nucleotide phosphodiesterase inhibitors: Shifting the focus from inotropy to cyclic adenosine monophosphate. *J. Am. Coll. Cardiol.* **34**(2), 318–324 (1999).
54. Yang, Z. *et al.* A dominant role for FE65 (APBB1) in nuclear signaling. *J. Biol. Chem.* **281**(7), 4207–4214 (2006).
55. Schettini, G. *et al.* Phosphorylation of APP-CTF-AICD domains and interaction with adaptor proteins: Signal transduction and/or transcriptional role–relevance for Alzheimer pathology. *J. Neurochem.* **115**(6), 1299–1308 (2010).
56. Sauvageau, E. *et al.* CNIH4 interacts with newly synthesized GPCR and controls their export from the endoplasmic reticulum. *Traffic* **15**(4), 383–400 (2014).
57. Liu, Q. *et al.* Monocyte to macrophage differentiation-associated (MMD) positively regulates ERK and Akt activation and TNF-alpha and NO production in macrophages. *Mol. Biol. Rep.* **39**(5), 5643–5650 (2012).
58. Li, W. & He, F. Monocyte to macrophage differentiation-associated (MMD) targeted by miR-140-5p regulates tumor growth in non-small cell lung cancer. *Biochem. Biophys. Res. Commun.* **450**(1), 844–850 (2014).
59. Koyama, H. *et al.* Significance of tumor-associated stroma in promotion of intratumoral lymphangiogenesis: Pivotal role of a hyaluronan-rich tumor microenvironment. *Am. J. Pathol.* **172**(1), 179–193 (2008).
60. Bernert, B., Porsch, H. & Heldin, P. Hyaluronan synthase 2 (HAS2) promotes breast cancer cell invasion by suppression of tissue metalloproteinase inhibitor 1 (TIMP-1). *J. Biol. Chem.* **286**(49), 42349–42359 (2011).
61. Ghosh, S. *et al.* Cannabinoid receptor CB2 modulates the CXCL12/CXCR4-mediated chemotaxis of T lymphocytes. *Mol. Immunol.* **43**(14), 2169–2179 (2006).
62. McCleland, M. L. *et al.* Lactate dehydrogenase B is required for the growth of KRAS-dependent lung adenocarcinomas. *Clin. Cancer Res.* **19**(4), 773–784 (2013).
63. Kummel, D. *et al.* The structure of the TRAPP subunit TPC6 suggests a model for a TRAPP subcomplex. *EMBO Rep.* **6**(8), 787–793 (2005).
64. Kim, J. J., Lipatova, Z. & Segev, N. TRAPP complexes in secretion and autophagy. *Front. Cell. Dev. Biol.* **4**, 20 (2016).
65. Peng, S. L. *et al.* NFATc1 and NFATc2 together control both T and B cell activation and differentiation. *Immunity* **14**(1), 13–20 (2001).
66. Rengarajan, J., Tang, B. & Glimcher, L. H. NFATc2 and NFATc3 regulate T(H)2 differentiation and modulate TCR-responsiveness of naive T(H)cells. *Nat. Immunol.* **3**(1), 48–54 (2002).
67. Kass, D. A., Champion, H. C. & Beavo, J. A. Phosphodiesterase type 5: Expanding roles in cardiovascular regulation. *Circ. Res.* **101**(11), 1084–1095 (2007).
68. Li, S., et al., Phosphodiesterase-5a knock-out suppresses inflammation by down-regulating adhesion molecules in cardiac rupture following myocardial infarction. *J. Cardiovasc. Transl. Res.* (2021).
69. Lahoz, A. & Hall, A. DLC1: A significant GAP in the cancer genome. *Genes Dev.* **22**(13), 1724–1730 (2008).
70. Shih, Y. P., Yuan, S. Y. & Lo, S. H. Down-regulation of DLC1 in endothelial cells compromises the angiogenesis process. *Cancer Lett.* **398**, 46–51 (2017).
71. Page, N. *et al.* Persistence of self-reactive CD8+ T cells in the CNS requires TOX-dependent chromatin remodeling. *Nat. Commun.* **12**(1), 1009 (2021).
72. Aliahmad, P. *et al.* TOX is required for development of the CD4 T cell lineage gene program. *J. Immunol.* **187**(11), 5931–5940 (2011).
73. Kaneda, M. M. *et al.* PI3Kgamma is a molecular switch that controls immune suppression. *Nature* **539**(7629), 437–442 (2016).
74. Sasaki, T. *et al.* Function of PI3Kgamma in thymocyte development, T cell activation, and neutrophil migration. *Science* **287**(5455), 1040–1046 (2000).
75. Nandagopal, N. *et al.* The critical role of IL-15-PI3K-mTOR pathway in natural killer cell effector functions. *Front. Immunol.* **5**, 187 (2014).
76. Sutton, M. N. *et al.* DIRAS3 (ARHI) blocks RAS/MAPK signaling by binding directly to RAS and disrupting RAS clusters. *Cell. Rep.* **29**(11), 3448–3459 (2019).
77. Corral-Serrano, J. C. *et al.* PCARE and WASF3 regulate ciliary F-actin assembly that is required for the initiation of photoreceptor outer segment disk formation. *Proc. Natl. Acad. Sci. USA* **117**(18), 9922–9931 (2020).

Author contributions

J.v.N. wrote the main manuscript text and performed the experiments. K.S. performed the analysis in the independent dataset; M.v.d.B. and A.F. are the primary supervisors; C.-A.B. and W.T. are the secondary supervisors. M.v.d.B. was involved in obtaining the NORM dataset; W.T. and P.H. were involved in obtaining the GLUCOLD dataset. All authors reviewed the manuscript.

Competing interests

The authors declare no competing interests.

Additional information

Supplementary Information The online version contains supplementary material available at https://doi.org/10.1038/s41598-022-09093-0.

Correspondence and requests for materials should be addressed to M.B.

Reprints and permissions information is available at www.nature.com/reprints.

Publisher's note Springer Nature remains neutral with regard to jurisdictional claims in published maps and institutional affiliations.